Arab J. Nucl. Sci. Appl., Vol. 56, 3, 155-165 (2023)

ISSN 1110-0451

Arab Journal of Nuclear Sciences and Applications

Web site: ajnsa.journals.ekb.eg

(E S N S A)

Possible Quasi-periodic Oscillation in the Distant γ-Ray Blazar PKS 0454–234

Y. Abdou[(1)*], M.A. Hashad[(1,2)], I.I. Boundok[(1)], Amr A. El-Zant[(3)]

[(1)]*Physics Department, Faculty of Science, Tanta University, Tanta, Egypt*
[(2)]*Basic Science Department, Modern Academy for Engineering and Technology, Cairo, Egypt*
[(3)]*Center for Theoretical Physics, The British University in Egypt, Cairo*

ARTICLE INFO

Article history:

Received: 24th Aug. 2022
Accepted: 6th Nov. 2022

Keywords:

Active galactic nuclei;
Quasi-periodicity;
Non-thermal radiation mechanisms;
Gamma-rays.

ABSTRACT

An important observational feature of *Fermi*-LAT blazars is their variability, which remarkably occasionally shows quasi-periodic oscillations (QPOs); a characteristic that could convey information regarding the emission mechanism from their central engines, as well as the possibility of observing merging systems. This work searches for 0.1–100 GeV γ-ray periodic modulations in the distant ($\mathrm{redshift} = 1.003$) flat-spectrum radio quasar PKS 0454–234, using the *Fermi*-LAT pass 8 data for time span of about 14 yr. The search for such signals in the γ-ray light curves was carried out using four methods: the Generalized Lomb-Scargle periodogram (GLSP), the weighted wavelet z-transform (WWZ), the REDFIT algorithm, as well as the auto-correlation function. Two possible QPO signals were found with periods of 3.51 ± 0.33 yr and 6.10 ± 0.82 yr, at the significance levels of ~4σ and ~3σ, respectively. Even though the latter periodicity is less significant than the former, it in fact gives a better fit to the fluxes. Considering a super binary black hole system (SBBHS) model, the parameters of the binary were estimated (for the period of 6 yr) as follows: a binary separation of $R \sim 0.005$ pc, with total mass $M \sim 4.69 \times 10^8\ \mathrm{M}_\odot$, and decay time of the gravitational wave emission $T_{GW} \sim 9.56 \times 10^4$ yr.

1. INTRODUCTION

Blazars are a category of active galactic nuclei (AGNs) with relativistic plasma jet almost oriented toward the Earth ($\theta < 5°$) [1-4]. The non-thermal emission of gamma-ray blazars is often characterized by erratic variability over a wide range in both the spectral and temporal domains. Blazars are also known to own extreme properties [2, 5]; for instance being the most luminous sources ($L \sim 10^{47} \mathrm{erg\ s^{-1}}$) are endowed with supermassive black holes (SMBHs) $> 10^6\ \mathrm{M}_\odot$ driving their central engine, and their emission is generally characterized by flux and polarization variability.

Generally speaking, the spectral energy distribution of blazars has two humps. The infrared to X-ray energy peak is dominated by synchrotron emission. According to leptonic model [6], the MeV to GeV peak is the results of inverse Compton scattering of the low energy synchrotron photons and/or ambient photons (e.g., from broad-line region, the accretion disc, or dusty torus) [7, 8]. Blazars are typically classified into two subclasses according to the emission line features of the optical band. The first subclass is termed flat spectrum radio quasars (FSRQs) which have strong emission lines and the second subclass is BL Lac objects which have weak or even absent emission lines [1]. The FSRQ γ-ray emission is usually generated by the external Compton mechanism.

The study of the violent time variation, including in the profile of light curves (LCs) and in the variability timescale, puts constraints on the jet physics. Quasi-periodic oscillation studies of blazars, in particular, could in addition embody evidence of binary SMBH systems [9-11]. In spite of the fact that the variability of blazars generally appears to be aperiodic [12-15], several studies have searched for quasi-periodic variation (e.g.,

Corresponding author: yasser.abdou@science.tanta.edu.eg
DOI: 10.21608/ajnsa.2022.158331.1629

[9, 15-27]). The geometrical origins for the periodicity of γ-ray blazars include, but not limited to, jet precession, helical structures in the jet, or intrinsic jet rotation [22, 25, 28-30]. According to Λ cold dark matter (CDM) model of structure formation, galaxies evolve and grow in halo potential wells through accretion of smaller substructures and major mergers (e.g. [31]). In this context, the SMBH's at their centers are also expected to merge, as the separation distance of the SMBHs gradually shrinks, the gravitational bound becomes harder [32]. The rate of such events is expected to sharply increase with redshift, as mergers, particularly major mergers, become more frequent [33]. These mergers are furthermore more likely to be between gas rich galaxies, and therefore lead to significant central engine emission, which may be detectable through the on board *Fermi*-LAT all-sky monitoring telescope that provides the opportunity to perform an exploration for cyclical γ-ray sources [34].

In this study, we performed a long-term study of the distant FSRQ PKS 0454–234 based on the γ-ray data from the *Fermi*-LAT since the start of its mission in 2008 August to 2022 June. This paper is organized as follows. In Section 2 we describe the details of the *Fermi*-LAT data analysis. Section 3 presents the results, which are discussed and summarized in Section 4.

2. Observations and Data Reduction

The Space-based Gamma ray Fermi Large Area Telescope (LAT) is a pair conversion telescope that detects γ-rays, spanning an energy range that starts from below 20 MeV and goes up to 500 GeV. Since its launch on 11th June 2008, LAT has scanned the γ-ray sky every ~3 hours, and as such it has been regularly observing the emission of γ-ray from cosmic sources. For details on the *Fermi*-LAT instrument see [34].

We constructed light curves for the source PKS 0454–234 with the standard pass8 *ScienceTools*, which is accessible in the Fermi Science Support Center (FSSC)[1], using the instrument response functions P8R2_SOURCE_V6 of P8R3_SOURCE class photons. The light curves cover about ~14 yr, from 2008 August 4 to 2022 June 22 (MJD 54682.66–59752.66), with an energy ranges from 100 MeV to 100 GeV. The events are picked within region of interest (ROI) of a 12° in radius centered on the location of the source. The chosen ROI is to reflect the radius of 95% containment of the LAT point-spread function at 100 MeV. Additional data selection cuts are applied to reject photons associated with periods and regions of known GRB activity and solar flare, as well as a zenith angle cut of 90° to avoid γ-rays contamination from the Earth limb caused by cosmic rays interactions with Earth's atmosphere.

In addition to the 4FGL-DR2 catalog of point sources[2], isotropic and Galactic background components are also involved in the XML model, which provides a better description to the observed photon distribution to be used in the maximum likelihood optimization. We use the 'gll_iem_v07.fits' Galactic component, which is a spatial and spectral template of the Milky Way's interstellar diffuse γ-ray emission, and the 'iso_P8R3_SOURCE_V3_v1' isotropic component, which provides a spectral template to represent all remaining isotropic emission. It contains contributions from both the isotropic celestial γ-ray emission and residual charged-particle backgrounds.

The normalization of the source spectrum and the normalization of the variable sources in the ROI are left free to be varied in the model, while the spectral parameters of the variable sources in the ROI are frozen to their catalog values. The test statistic (TS) threshold for a meaningful detection was set to 9 (~3σ) (defined as $TS = -2\ \ln(L_0/L_1)$. An unbinned maximum likelihood algorithm is applied using '*gtlike'* between the events of observation and the model file.

3. RESULTS

3.1. γ-ray Light Curves

The source 4FGL J0457.0–2324 (counterpart name: PKS 0454–234) is a distant blazar located at redshift $z = 1.003$ [35] with RA $= 74.26$ degree and Dec $= -23.41$ degree. It was classified as a soft spectrum FSRQ [36], though it is bright at the high energy γ-ray regime. According to the LAT 4th catalog, spanning 10 years of observations, its average integral Flux is $F_{1000} = 1.81 \times 10^{-8} \pm 2.10 \times 10^{-10}$ photons cm^{-2} s^{-1}. It has a predicted number of photons $N_{pred} = 24240.38$ with average test statistics TS $= 53020$, and flux fractional variability $F_{var} = 48.29 \pm 11.41\%$ [37]. High activity of γ-rays from the object was reported few times, and was also followed up in radio and near infrared [21, 36, 38, 39].

[1] http://fermi.gsfc.nasa.gov/ssc/data/analysis/scitools/

[2] https://fermi.gsfc.nasa.govimes/ssc/data/access/lat/10yr_catalog/

We constructed high energy γ-ray light curves for PKS 0454–234 using monthly (Fig. 1) and weekly (Fig. 2) time binning, with the unbinned maximum likelihood method within energy range 0.1–100 GeV for about 14 yr. The two different time binnings are used in this analysis to test the effect of binning on the quasi-periodicity properties. The change of time interval does not lead to a major difference in the LCs patterns but has a clear impact on the periodicity analysis. There is an obvious variability in the observed γ-ray fluxes and their corresponding photon spectral indices, where the average fluxes are $F_{av} = 2.56 \times 10^{-7} \pm 1.2 \times 10^{-8}$ photons cm^{-2} s^{-1} and $F_{av} = 2.65 \times 10^{-7} \pm 0.6 \times 10^{-8}$ photons cm^{-2} s^{-1} for monthly and weekly LCs, respectively.

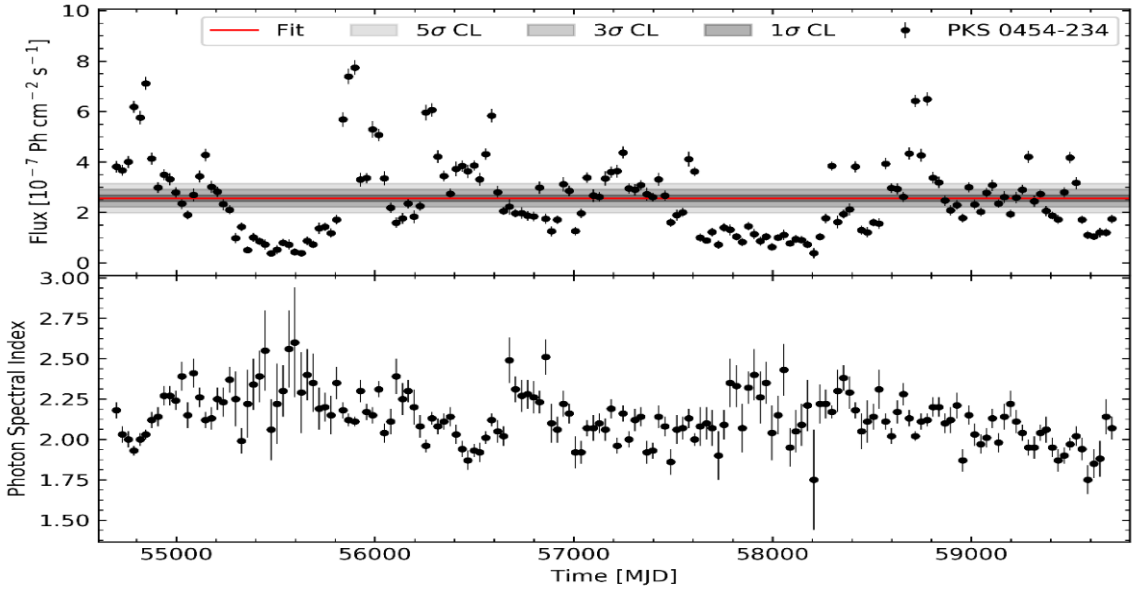

Fig. (1): Monthly binned γ-ray light curve of the source PKS 0454–234 during the period from August 2008 to June 2022, showing photon flux (top panel) and γ-ray spectral index (bottom panel). The energy range is between 100 MeV and 100 GeV. The red solid line represents a fit with a constant, $F_{av} = 2.56 \times 10^{-7} \pm 1.2 \times 10^{-8}$ photons cm^{-2} s^{-1}. The confidence intervals 1σ, 3σ, and 5σ of the constant function fit are indicated by the gray shaded regions. The vertical error bars are the one-sigma error bars.

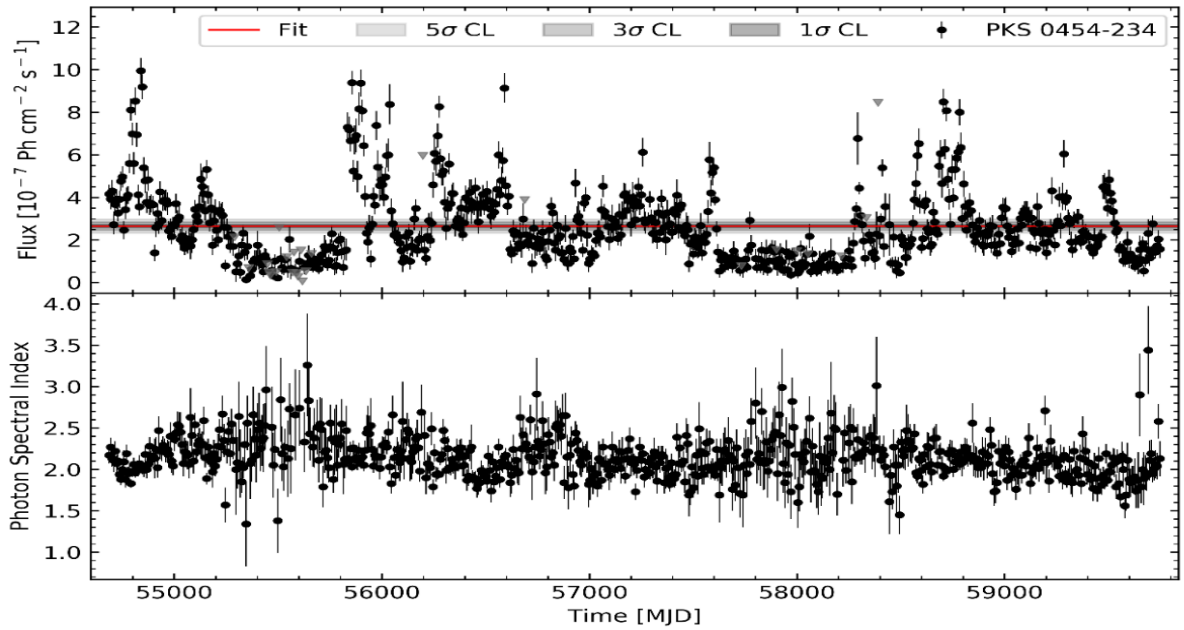

Fig. (2): Weekly binned γ-ray light curve of the source PKS 0454–234 from August 2008 to June 2022 in the energy range between 100 MeV and 100 GeV, showing photon flux (top panel) and γ-ray spectral index (bottom panel). Filled black points denote significant detections, downward grey arrows denote 95% confidence level upper limits. The threshold of the detection is set at TS > 9, where the photon index is only plotted. The red solid line represents a fit with a constant, $F_{av} = 2.65 \times 10^{-7} \pm 0.6 \times 10^{-8}$ photons cm^{-2} s^{-1}. The confidence intervals 1σ, 3σ, and 5σ of the constant function fit are presented with the gray shaded regions. Vertical error bars are the one-sigma error bars.

3.2. Flux Distribution

The probability density function (PDF) of the time series is an essential property for the study of blazars. It may embody important information regarding the blazar central engine, and help to constrain the underlying physical process driving the variability (e.g., [40]; [41]; [9]). Particularly, the PDF statistics of high energy γ-rays can provide vital insights on its emission processes nature [5]. One can estimate the PDF by fitting a model function to a histogram assembled from the long-term LC photon fluxes. Current findings suggest that the blazars' γ-ray fluxes are preferentially log-normally distributed [42]. Consequently, multiplicative processes for the origin of blazar variability become favorable, compared to additive models (e.g., a simple many "mini-jets" superposition or shot-noise). Several scenarios for the cause of log-normal flux distributions are suggested such as the multiplicative behavior as a result of accretion disk fluctuations [43, 44] and the acceleration process of particle itself [41]; more details can also be found in [9, 42].

The PKS 0454–234 γ-ray photon fluxes distribution was fitted by log-normal L(ϕ) and Gaussian G(ϕ) distribution functions given by:

$$L(\varphi|\mu,\sigma) = \frac{1}{\sqrt{2\pi}\sigma\varphi}\exp\left(-\frac{(log(\varphi)-\mu)^2}{2\sigma^2}\right) \quad \textbf{(1)}$$

and

$$G(\varphi|\mu,\sigma) = \frac{1}{\sqrt{2\pi}\sigma}\exp\left(-\frac{(\varphi-\mu)^2}{2\sigma^2}\right) \quad \textbf{(2)}$$

respectively, where μ is the mean of the distribution and σ is its standard deviation. Fig. 3 shows the flux histogram with best-fitting results. The error bars of the frequency bins show the Poisson estimation given by Gehrels (1986) [45]. The log-normal PDF gives a better representation of the flux distribution to the Gaussian PDF. The Gaussian and log-normal fit parameters and R^2 test are listed in Table (1).

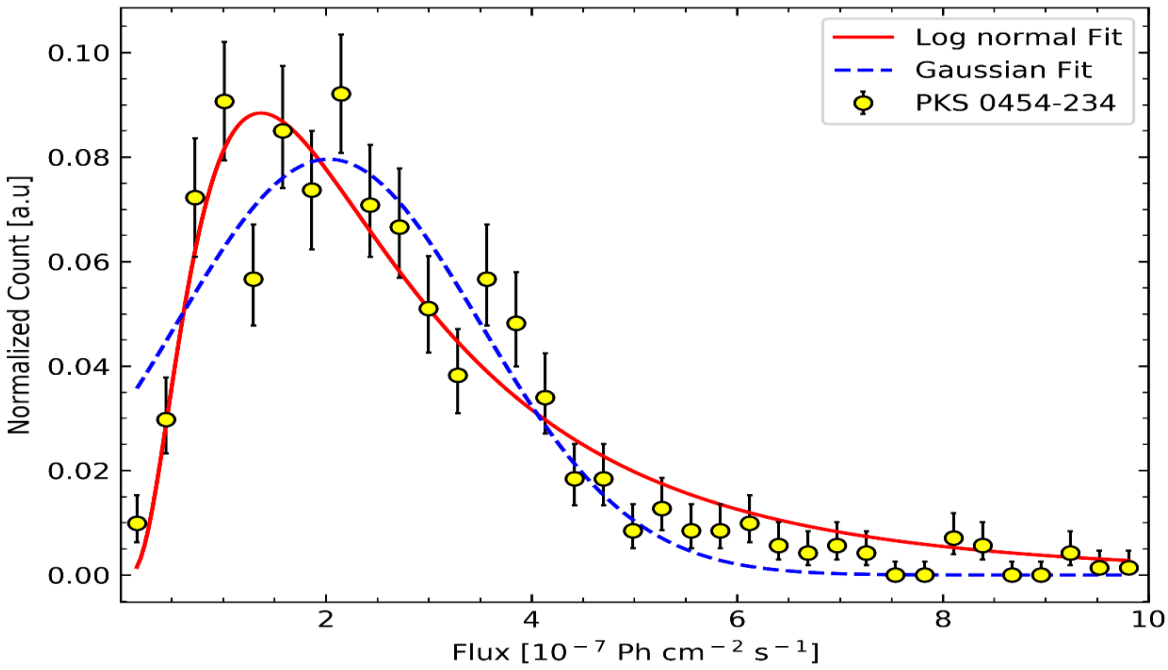

Fig. (3): Normalized histogram of γ-ray fluxes fitted with a log-normal (solid red line), and Gaussian (dashed blue line), respectively. PKS 0454–234 expresses a strong preference for log-normal distribution.

Table (1): Fit parameters of PKS 0454–234 PDF to the log-normal distribution and the Gaussian distribution as well as its flux normality test.

Time bin	*Log-normal*			*Gaussian*			*Normality test (Shapiro-Wilk)*
	μ*	σ*	R^2	μ*	σ*	R^2	P < 0.001
7 day	2.40	0.75	0.91	2.03	1.47	0.89	W-Statistic = 0.903

Notes. *In units of $\times 10^{-7}$ photon cm^{-2} s^{-1}.

3.2. Searching for γ-ray periodicity

3.2.1. Lomb–Scargle periodogram

The Lomb–Scargle periodogram (LSP) is well-known algorithm for periodicity detection and characterization in astronomical time-series [46, 47], regardless of whether the time series data is evenly spaced or has gaps and irregularities. The standard normalized LSP basically attempts to attain a least square fit for sinusoidal waves of the form $y(t) = A\cos(\omega t) + B\sin(\omega t)$ to the time series. It is given, for a time series (t_i, y_i), by

$$P(\omega) = \frac{1}{2}\left\{\frac{(\sum_i y_i \cos\omega(t_i-\tau))^2}{\sum_i cos^2\,\omega(t_i-\tau)} + \frac{(\sum_i y_i \sin\omega(t_i-\tau))^2}{\sum_i sin^2\,\omega(t_i-\tau)}\right\},$$

where τ is specified for each frequency, in order to guarantee time-shift invariance. It is given by,

$$\tau = \frac{1}{2\omega}\, tan^{-1}\left(\frac{\sum_i \sin(2\omega t_i)}{\sum_i \cos(2\omega t_i)}\right) \qquad (3)$$

The choice of LSP frequency grid is a critical decision, particularly for nonuniform data. Thus, we set the minimum frequency to be a one oscillation cycle $1/T$ which match the whole time of observation T. The maximum frequency was set to Nyquist frequency, $\nu_{max} = 1/(2\Delta t)$, in order not to miss any relevant information. To ensure that the grid suitably samples each peak, avoiding consuming unnecessarily long computation times, the total number of sample frequencies of periodogram can be empirically set as $N_\nu = n_o T \nu_{max}$, with samples per peak n_0 in the range of 5–10 [48]. The Generalized Lomb–Scargle periodogram has also been applied to the LCs. The GLSP has the advantage of taking measurement errors into account. It adds to the fitting sinusoidal wave an offset 'c', i.e. $y(t) = A\cos(\omega t) + B\cos(\omega t) + c$ [49]. In the γ-ray blazars context, the contribution to the constant term is from the isotropic diffuse γ-ray background [21, 25]. Spurious peaks in the real astronomical observations can arise due to a number of factors [48]; e.g., window function aliasing and random variation in flux (white noise), and power leakage from the true peaks due to observations errors. Therefore, the estimated period uncertainty is an essential aspect when reporting the results of periodogram. To this end, false alarm probability (FAP) is a typical method used to estimate peak significance [49]. The FAP determines the probability that a color-noise aperiodic time series exceeds a certain power level caused by coincidental alignment in the random fluctuations [16, 21, 48].

Fig. (4) shows the Zechmeister-Kürster (ZK) periodogram associated with the best fitting sinusoidal wave to the monthly LC ($T = 6.14 \pm 0.09$ yr) and phase folded LC, which showed phase shift of 0.336 ± 0.01. For the monthly binning LC's ZK periodogram, the FAP for the maximum power (P[ZK] = 0.28) is 8.15×10^{-11}, with a chance probability of 9.92×10^{-13}. For the weekly binning, the FAP for the maximum power (P[ZK] = 0.46) is 1.26×10^{-15}, with a chance probability of $< 10^{-15}$. An alternative method to infer power peak significance is built on simulating LCs [16, 20, 50]. Using Emmanoulopoulos' method [51], as coded in Python by [52], 5×10^4 LCs were simulated, matching both the PSD and the PDF of PKS 0454–234 LC. For each simulated LC, a GLSP was applied, and the percentile was determined for each period to estimate the power confidence level.

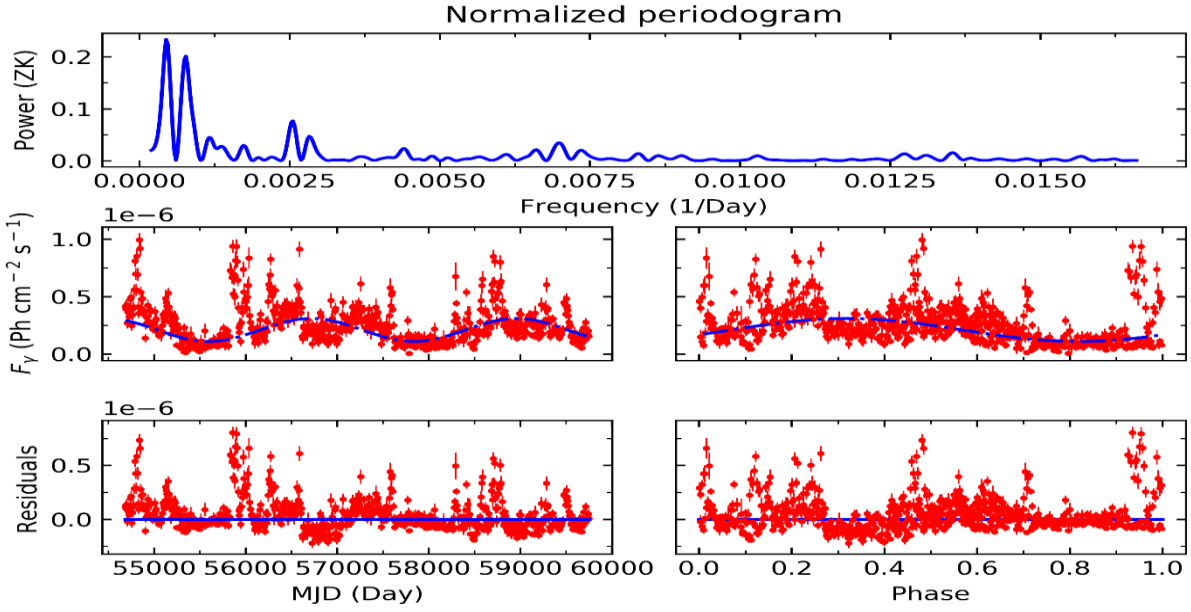

Fig. (4): ZK periodogram (upper panel) associated with the best fitting sinusoidal wave (the blue curve) to the LC data (the red points), with best sine period of $T = 6.14 \pm 0.09$ yr (the middle left panel). Middle right panel shows the phase folded (the red points) of the best periodicity signal (the blue curve) with phase shift $= 0.336 \pm 0.01$. The lower panel shows the residuals of the sinusoidal and phase fits, respectively.

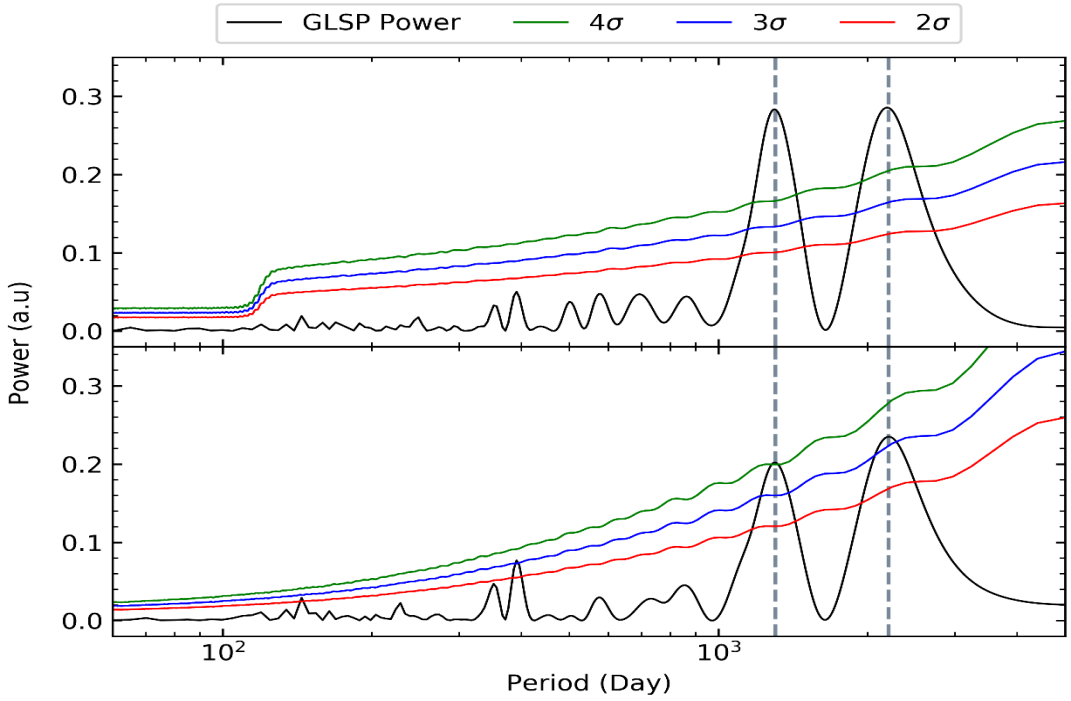

Fig. (5): Upper and lower panel are the GLSPs of PKS 0454–234 γ-ray LCs for about ~14 yr, with monthly and weekly time binning, respectively. The GLSPs are shown in black lines. The green, blue, and red lines present the 4σ, 3σ, 2σ confidence levels, respectively, which are calculated through simulations of 50,000 LCs using Emmanoulopoulos' method [51].

The GLSPs of the monthly and the weekly PKS 0454–234 LCs are shown in Fig. (5). One peak was identified with period 3.53 ± 0.34 yr, with significance $\sim 7.3\sigma$ in the monthly LC, and 3.51 ± 0.33 yr with significance 3.93σ in the weekly LC. Another peak was identified with period 6.05 ± 0.77 yr, with significance of 5.94σ in the monthly LC and 6.10 ± 0.82 yr, with significance 3.12σ, in the weekly LC. By fitting the power peak to a Gaussian peak, the period was estimated and its uncertainty is the fitting's half width at half maximum (HWHM). The choice of LC time binning as well as existence of gaps in the data affect the GLSP results. However, the period of 6.10 yr is less significant than the period of 3.51 yr (where the periodicity of 6.10 yr in period is corresponding to 2.3 cycles over the available *Fermi*-LAT data), the 6.10 yr period gave the best fit to the fluxes which encourages long-term of observations to improve the significance in the future.

3.2.2. Weighted wavelet z-transform

A powerful tool for analyzing the periodicity is the weighted wavelet z-transform [53] , which fits unevenly spaced sampling light curves to sinusoidal functions. The WWZ power is computed as a function of observing time and frequency. In this sense, the WWZ is superior to GLSP; in accounting for possible transient nature of the QPOs. Its peaks illustrate the duration as well as the strength of a possible QPOs [24, 30]. The two possible quasi-periodicity signals discussed above have also been identified by the WWZ method, as shown in Fig. (6).

3.2.3. REDFIT and auto-correlation function

As blazars LCs typically come with strong red noise, this has led to skepticisms toward claims of QPOs detection in blazars [5]. We therefore also applied another method for detecting periodicity, namely REDFIT [54], which uses a first order autoregressive (AR1) process for the fitting to estimate the red-noise spectrum. The significance of the peaks in the PSD can be precisely assessed against the background red-noise with this method, which was used to detect periodicity in the weekly binned LC (using the REDFIT3.8e[3] package; with analysis criteria described here [17]). The results suggest the two aforementioned periodicities at significances exceeding 95% (Fig. 7). We note that the REDFIT maximum significance could be provided is only 2.5σ. Finally, the auto-correlation function of the monthly binning LC detected two periods of ~3.12 yr (~2σ) and ~6.60 yr (~3σ) as shown in Fig. (8).

[3] https://www.marum.de/Prof.-Dr.-michael-schulz/Michael-Schulz-Software.html

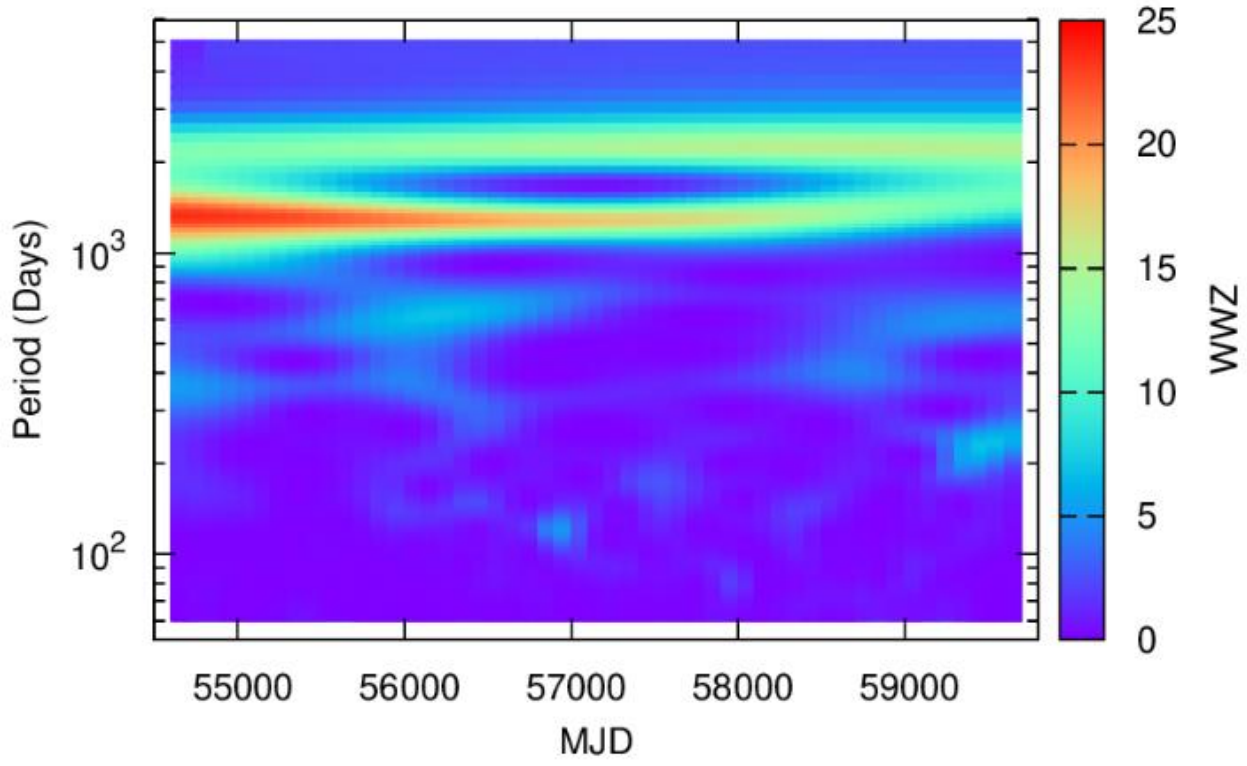

Fig (6): 2D plane contour of the WWZ power of the weekly PKS 0454–234 γ-ray light curve.

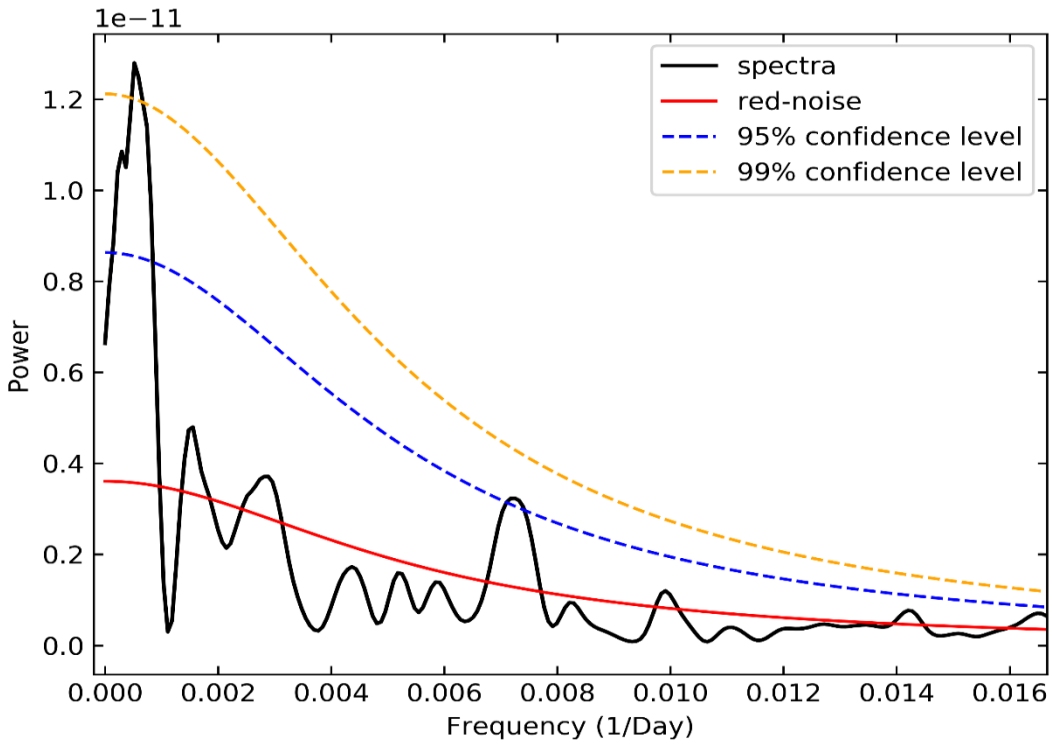

Fig. (7): REDFIT periodicity analysis results: power spectrum (black line), spectrum of theoretical red-noise (red line), 95% confidence level (blue dashed line), and 99% confidence level (orange dashed line).

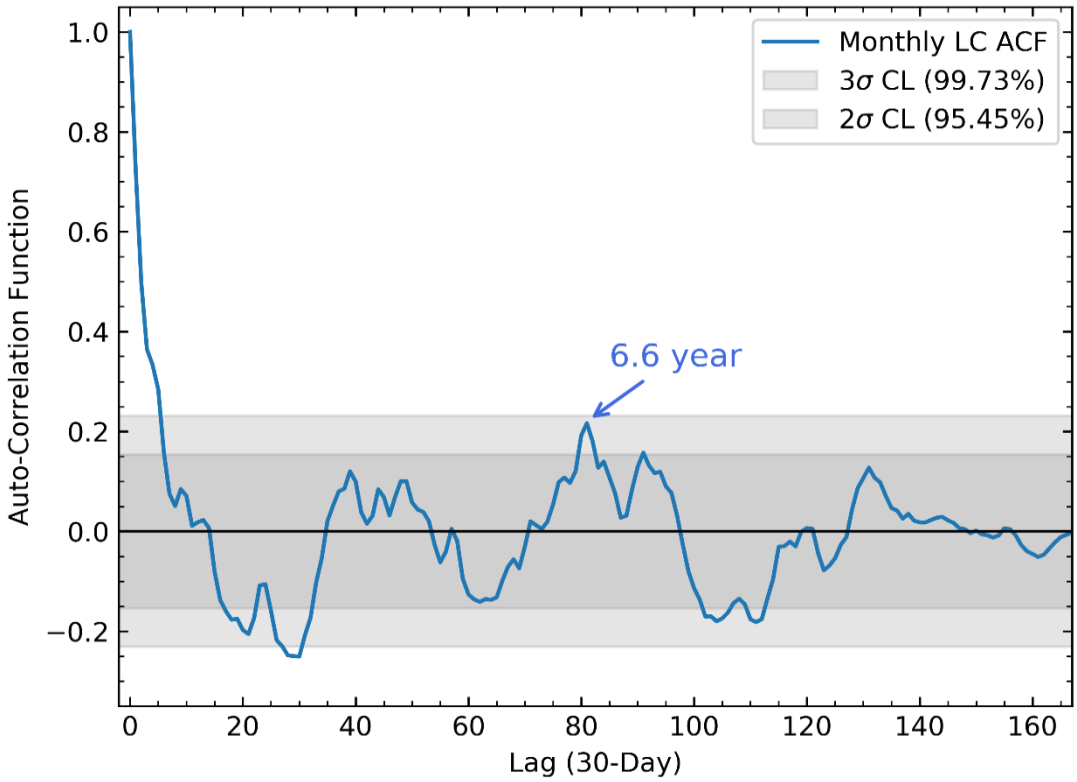

Fig. (8): Auto-correlation function of the monthly γ-ray LCs of 0.1–100 GeV energy range, likelihood in the blue line and aperture photometry in the orange line, where the gray shadings are the 95.45% and 99.73% confidence limits of the white noise.

3. Summary and Discussions

Searches for periodicities in the *Fermi*-LAT blazars light-curves have constituted an active topic of research, particularly after the first evidence (at ~3σ) for periodic modulation [25] of 2-years in the blazar PG 1553+113 LC [9, 11, 15-17, 20, 23]. Due to the limited monitoring duration of the *Fermi*-LAT satellite, caution should be taken and significance assessment against a white-noise background conducted [18, 55]. The identification of γ-ray QPOs in blazars, on the other hand, can definitely shed light on their high-energy emission processes nature. And while the significance of the observations are being investigated, different scenarios explaining the tentative data have been presented. These include: jet precision, accretion disk instabilities, and existence of supermassive binary black hole systems [5].

In the present work, a full temporal analysis was carried out for the distant blazar PKS 0454–234 (redshift = 1.003) searching for possible periodicity in the *Fermi*-LAT high energy γ-ray data from 2008 August to 2022 June. The γ-ray monthly and weekly LCs were extracted using maximum likelihood technique in the 100 MeV–100 GeV energy range. An obvious variability was noticed in the LCs' fluxes and their corresponding photon spectral indices as well where $F_{av} = 2.56 \times 10^{-7} \pm 1.2 \times 10^{-8}$ photons cm^{-2} s^{-1} and $F_{av} = 2.65 \times 10^{-7} \pm 0.6 \times 10^{-8}$ photons cm^{-2} s^{-1} for monthly and weekly LCs, respectively.

The spectra of FSRQs generally appear soft with photon spectral index $\Gamma_\gamma > 2$ [56]. However, PKS 0454–234 was observed to have ~hard intrinsic γ-ray spectrum (Γ ~2.1), particularly at the active periods of the high energy gamma rays. Therefore, the object can possibly be detected by the very high energy observatories. As a log-normal distribution provides a better fit to the PDF of γ-ray fluxes, compared with a Gaussian, the PDF of the PKS 0454–234, as with most LAT blazars, the underlying variability could be a result of a nonlinear, multiplicative process.

Two possible quasi-periodic modulations were detected in the LC. One with a period of 3.51 ± 0.33 yr, with a significance of 3.93σ; the second at a period of 6.10 ± 0.82 yr, with a significance of 3.12σ. The periodicity analysis is affected by the existence of gaps in the data, the time binning, and indeed the choice of time intervals of the LC. The 2.3 cycle for the period of 6.10 yr gives poor significance, which motivates the use of longer term observations to confirm the results in the future.

As already mentioned, there are different explanations for apparent periodic signals in blazars. Given the relatively high redshift of our source, coming from a phase in cosmic history when the halo (and therefor galaxy and SMBH) merging rate is expected to be significantly higher than at present, we entertain in particular the merging binary scenario. In this context, the parameters of the binary were calculated (for the period of 6 yr; cf. Appendix). Such a binary was estimated to have separation $R \sim 0.005$ pc, with total mass $M \sim 4.69 \times 10^8$ $M_\odot$, and gravitational wave emission decay time $T_{GW} \sim 9.56 \times 10^4$ yr.

Software: Fermitools[4], NumPy [57], Matplotlib [58], PyAstronomy [59], DELCgen-Simulating light curves [52], REDFIT [54].

REFERENCES

[1] Urry, C.M. and P. Padovani, *Unified schemes for radio-loud active galactic nuclei.* Publications of the Astronomical Society of the Pacific, 1995. **107**(715): p. 803.

[2] Françoise, C., Active Galactic Nuclei Fueling and feedback. IOP, 2021.

[3] Vovk, I. and A. Neronov, *Variability of gamma-ray emission from blazars on black hole timescales.* The Astrophysical Journal, 2013. **767**(2): p. 103.

[4] Boettcher, M. and J. Chiang, *X-ray spectral variability signatures of flares in BL Lacertae objects.* The Astrophysical Journal, 2002. **581**(1): p. 127.

[5] Bhatta, G. and N. Dhital, *The nature of γ-ray variability in blazars.* The Astrophysical Journal, 2020. **891**(2): p. 120.

[6] Finke, J.D., C.D. Dermer, and M. Böttcher, *Synchrotron self-Compton analysis of TeV X-ray-selected BL Lacertae objects.* The Astrophysical Journal, 2008. **686**(1): p. 181.

[7] Sikora, M., M.C. Begelman, and M.J. Rees, *Comptonization of diffuse ambient radiation by a relativistic jet: The source of gamma rays from blazars?* The Astrophysical Journal, 1994. **421**: p. 153-162.

[8] Kang, S.-J., L. Chen, and Q. Wu, *Constraints on the minimum electron Lorentz factor and matter content of jets for a sample of bright Fermi blazars.* The Astrophysical Journal Supplement Series, 2014. **215**(1): p. 5.

[9] Benkhali, F.A., et al., *Evaluating quasi-periodic variations in the γ-ray light curves of Fermi-LAT blazars.* Astronomy & Astrophysics, 2020. **634**: p. A120.

[10] Thiersen, H., M. Zacharias, and M. Böttcher, *Characterising the long-term variability of blazars in leptonic models.* Galaxies, 2019. **7**(1): p. 35.

[11] Tavani, M., et al., *The blazar PG 1553+ 113 as a binary system of supermassive black holes.* The Astrophysical Journal, 2018. **854**(1): p. 11.

[12] Hashad, M., et al., *Long-term and flares variability of Fermi LAT FSRQ 4C+ 21.35.* Arab Journal of Nuclear Sciences and Applications, 2019. **52**(2): p. 54-61.

[13] Badran, H., A. Basuny, and Y. Abdou, *Long-Term Time Variability of The Te V Blazer Mrk421 at High-Energy Using Fermi-LAT Measurements.* Isotope and Radiation Research, 2016. **48**(2): p. 171-195.

[14] Angioni, R., et al., *The large gamma-ray flare of the flat-spectrum radio quasar PKS 0346− 27.* Astronomy & Astrophysics, 2019. **627**: p. A140.

[15] Zhang, P.-f., et al., *Possible quasi-periodic modulation in the z= 1.1 gamma-ray blazar PKS 0426–380.* The Astrophysical Journal, 2017. **842**(1): p. 10.

[16] Peñil, P., et al., *Systematic search for γ-ray periodicity in active galactic nuclei detected by the Fermi Large Area Telescope.* The Astrophysical Journal, 2020. **896**(2): p. 134.

[17] Zhang, H., et al., *A Quasi-periodic Oscillation in the γ-Ray Emission from the Non-blazar Active Galactic Nucleus PKS 0521-36.* The Astrophysical Journal, 2021. **919**(1): p. 58.

[4] https://github.com/fermi-lat/Fermitools-conda

[18] Covino, S., A. Sandrinelli, and A. Treves, *Gamma-ray quasi-periodicities of blazars. A cautious approach.* Monthly Notices of the Royal Astronomical Society, 2019. **482**(1): p. 1270-1274.

[19] Zhou, J., et al., *A 34.5 day quasi-periodic oscillation in γ-ray emission from the blazar PKS 2247–131*. Nature communications, 2018. **9**(1): p. 1-6.

[20] Zhang, P.-F., et al., *A γ-ray Quasi-periodic Modulation in the Blazar PKS 0301–243?* The Astrophysical Journal, 2017. **845**(1): p. 82.

[21] Prokhorov, D. and A. Moraghan, *A search for cyclical sources of γ-ray emission on the period range from days to years in the Fermi-LAT sky.* Monthly Notices of the Royal Astronomical Society, 2017. **471**(3): p. 3036-3042.

[22] Cavaliere, A., M. Tavani, and V. Vittorini, *Blazar jets perturbed by magneto-gravitational stresses in supermassive binaries.* The Astrophysical Journal, 2017. **836**(2): p. 220.

[23] Castignani, G., et al., *Multiwavelength variability study and search for periodicity of PKS 1510–089.* Astronomy & Astrophysics, 2017. **601**: p. A30.

[24] Bhatta, G., et al., *Detection of possible quasi-periodic oscillations in the long-term optical light curve of the BL Lac object OJ 287.* The Astrophysical Journal, 2016. **832**(1): p. 47.

[25] Ackermann, M., et al., *Multiwavelength evidence for quasi-periodic modulation in the gamma-ray blazar PG 1553+ 113.* The Astrophysical Journal Letters, 2015. **813**(2): p. L41.

[26] Kadler, M., et al., *A quasi-periodic modulation of the radio light curve of the blazar PKS B0048-097.* Astronomy & Astrophysics, 2006. **456**(2): p. L1-L4.

[27] Vaughan, S., et al., *On characterizing the variability properties of X-ray light curves from active galaxies.* Monthly Notices of the Royal Astronomical Society, 2003. **345**(4): p. 1271-1284.

[28] Sobacchi, E., M.C. Sormani, and A. Stamerra, *A model for periodic blazars.* Monthly Notices of the Royal Astronomical Society, 2016: p. stw2684.

[29] Rieger, F.M., *On the geometrical origin of periodicity in blazar-type sources.* The Astrophysical Journal, 2004. **615**(1): p. L5.

[30] Mohan, P. and A. Mangalam, *Kinematics of and emission from helically orbiting blobs in a relativistic magnetized jet.* The Astrophysical Journal, 2015. **805**(2): p. 91.

[31] White, S.D. and C.S. Frenk, *Galaxy formation through hierarchical clustering.* The Astrophysical Journal, 1991. **379**: p. 52-79.

[32] Begelman, M.C., R.D. Blandford, and M.J. Rees, *Massive black hole binaries in active galactic nuclei.* Nature, 1980. **287**(5780): p. 307-309.

[33] Tacconi, L., et al., *High molecular gas fractions in normal massive star-forming galaxies in the young Universe.* Nature, 2010. **463**(7282): p. 781-784.

[34] Atwood, W., et al., *The large area telescope on the Fermi gamma-ray space telescope mission.* The Astrophysical Journal, 2009. **697**(2): p. 1071.

[35] Stickel, M., J. Fried, and H. Kuehr, *Optical spectroscopy of 1 Jy BL Lacertae objects and flat spectrum radio sources.* Astronomy and Astrophysics Supplement Series, 1989. **80**: p. 103-114.

[36] Tsujimoto, S., et al. *Very-high-energy gamma-ray emission from high-redshift blazars with Fermi-LAT data in the southern hemisphere*. in *International Cosmic Ray Conference*. 2013.

[37] Abdollahi, S., et al., *Incremental Fermi Large Area Telescope Fourth Source Catalog.* arXiv preprint arXiv:2201.11184, 2022.

[38] Sacahui, J., et al., *Study of blazar activity in 10 year Fermi-LAT data and implications for TeV neutrino expectations.* Revista mexicana de astronomía y astrofísica, 2021. **57**(2): p. 251-268.

[39] Tsujimoto, S., et al., *Blazar Variability and Evolution in the GeV Regime.* arXiv preprint arXiv:1502.03015, 2015.

[40] Uttley, P., I. McHardy, and S. Vaughan, *Non-linear X-ray variability in X-ray binaries and active galaxies.* Monthly Notices of the Royal Astronomical Society, 2005. **359**(1): p. 345-362.

[41] Shah, Z., et al., *Log-normal flux distribution of bright Fermi blazars.* Research in Astronomy and Astrophysics, 2018. **18**(11): p. 141.

[42] Rieger, F.M., *Gamma-Ray Astrophysics in the Time Domain.* Galaxies, 2019. **7**(1): p. 28.

[43] Lyubarskii, Y.E., *Flicker noise in accretion discs.* Monthly Notices of the Royal Astronomical Society, 1997. **292**(3): p. 679-685.

[44] Arévalo, P. and P. Uttley, *Investigating a fluctuating-accretion model for the spectral-timing properties of accreting black hole systems.* Monthly Notices of the Royal Astronomical Society, 2006. **367**(2): p. 801-814.

[45] Gehrels, N., *Confidence limits for small numbers of events in astrophysical data.* The Astrophysical Journal, 1986. **303**: p. 336-346.

[46] Lomb, N.R., *Least-squares frequency analysis of unequally spaced data.* Astrophysics and space science, 1976. **39**(2): p. 447-462.

[47] Scargle, J.D., *Studies in astronomical time series analysis. II-Statistical aspects of spectral analysis of unevenly spaced data.* The Astrophysical Journal, 1982. **263**: p. 835-853.

[48] VanderPlas, J.T., *Understanding the lomb–scargle periodogram.* The Astrophysical Journal Supplement Series, 2018. **236**(1): p. 16.

[49] Zechmeister, M. and M. Kürster, *The generalised Lomb-Scargle periodogram-a new formalism for the floating-mean and Keplerian periodograms.* Astronomy & Astrophysics, 2009. **496**(2): p. 577-584.

[50] Zhang, P.-f., et al., *Revisiting Quasi-periodic Modulation in γ-Ray Blazar PKS 2155-304 with Fermi Pass 8 Data.* The Astrophysical Journal, 2017. **835**(2): p. 260.

[51] 51. Emmanoulopoulos, D., I. McHardy, and I. Papadakis, *Generating artificial light curves: revisited and updated.* Monthly Notices of the Royal Astronomical Society, 2013. **433**(2): p. 907-927.

[52] Connolly, S., *A Python Code for the Emmanoulopoulos et al.[arXiv: 1305.0304] Light Curve Simulation Algorithm.* arXiv e-prints, 2015: p. arXiv: 1503.06676.

[53] Foster, G., *Wavelets for period analysis of unevenly sampled time series.* The Astronomical Journal, 1996. **112**: p. 1709-1729.

[54] Schulz, M. and M. Mudelsee, *REDFIT: estimating red-noise spectra directly from unevenly spaced paleoclimatic time series.* Computers & Geosciences, 2002. **28**(3): p. 421-426.

[55] Vaughan, S., et al., *False periodicities in quasar time-domain surveys.* Monthly Notices of the Royal Astronomical Society, 2016. **461**(3): p. 3145-3152.

[56] Madejski, G. and M. Sikora, *Gamma-ray observations of active galactic nuclei.* Annu. Rev. Astron. Astrophys, 2016. **54**: p. 725-760.

[57] Harris, C.R., et al., *Array programming with NumPy.* Nature, 2020. **585**(7825): p. 357-362.

[58] Hunter, J.D., *Matplotlib: A 2D graphics environment.* Computing in science & engineering, 2007. **9**(03): p. 90-95.

[59] Czesla, S., et al., *PyA: Python astronomy-related packages.* Astrophysics Source Code Library, 2019: p. ascl: 1906.010.

Appendix: Estimation of SMBH binary parameters

According to [28] the parameters of the binary system could be estimated, e.g., the binary separation:

$$R = 1.3 \times 10^{16} \left(\frac{1+q}{q}\right) T_2 \left(\Delta\theta_{obs,5}\right) cm \sim 0.005 \text{ pc}, \quad (\mathbf{4})$$

and the total mass

$$M = 1.7 \times 10^{8} \left(\frac{1+q}{q}\right)^3 T_2 \left(\Delta\theta_{obs,5}\right)^3 \sim 4.69 \times 10^{8} \text{ M}_{\odot}, \quad (\mathbf{5})$$

where q is the mass ratio of the secondary SMBH to the primary SMBH, $T_2 \equiv T_{int}/2$ yr, and $\Delta\theta_{obs,5} \equiv \Delta\theta_{obs}/5^{\circ}$ and with intrinsic time $T_{int} = T_{obs}/(1+z) = 6.10\, yr/(1+1.003) = 3.05$ yr, oscillations viewing angle of order $\Delta\theta_{obs} \sim$ few degree, and $q \gtrsim 1$. With the assumption of circular orbit and the jet is carried by the secondary SMBH (i.e. $q \gtrsim 1$), the decay time of the gravitational wave emission of the binary SMBH is

$$T_{GW} = 3.9 \times 10^{4}\, q \left(\frac{q}{1+q}\right)^3 T_2 \left(\Delta\theta_{obs,5}\right)^{-5} \sim 9.56 \times 10^{4} \text{ yr}. \quad (\mathbf{6})$$